Fully Organic Integrated Arrays on Flexible Substrates for X-Ray Imaging

Pawel E. Malinowski[1,*], Abhishek Kumar[2], Date J.D. Moet[2], David Cheyns[1], Barry P. Rand[1], Jan-Laurens P.J. van der Steen[2], Kris Myny[1], Soeren Steudel[1], Matthias Simon[3], Gerwin Gelinck[2], and Paul Heremans[1,2]

[1]IMEC, Kapeldreef 75, B-3001 Leuven, Belgium
[2]Holst Centre, High Tech Campus 31, 5656 KN Eindhoven, The Netherlands
[3]Philips Research, High Tech Campus 34, 5656 AE Eindhoven, The Netherlands
[*]E-Mail: Pawel.Malinowski@imec.be, Tel.: +32 1628 1938, Fax: +32 1628 1097

Organic photodetectors (OPDs) show high detectivity even with ultrathin (submicron) active layers and enable fabrication on large area, flexible substrates. In this work, 32x32 pixel arrays are demonstrated, where the active layer based on evaporated small molecules (SubPc/C_{60}) is monolithically integrated with a pentacene thin-film transistor readout on foil. The imagers were designed to be sensitive in the wavelength range between 500 and 600 nm to match the output of a typical scintillator used for x-ray imaging. The mean dark current density is below 10^{-6} A/cm^2, with a linearly increasing photocurrent from irradiance of 3 µW/cm^2.

Organic semiconductors are well established in the display industry and are gaining importance for photovoltaic and electronic applications [1]. A major benefit of organic semiconductor technology is that it enables low-cost fabrication of devices on various substrates, such as silicon, glass, foil or CMOS circuits [2,3]. Using large-area, flexible foil substrates can lead to light-weight, rugged, bendable and conformable electronics.

In this work, organic photodetectors (OPDs) were fabricated using a planar heterojunction structure with a 20 nm thick subphthalocyanine (SubPc) donor layer and a 30 nm thick fullerene (C_{60}) acceptor layer [4,5]. The entire photodetector structure was thermally evaporated, yielding an ultrathin active stack with excellent uniformity (Fig. 1).

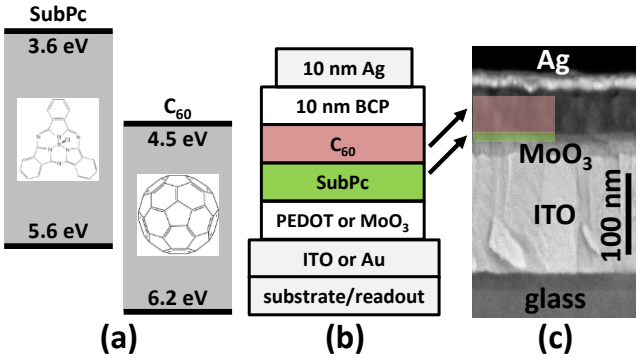

Figure 1. Energy diagram (a), layer stack (b) and scanning electron microscope cross-section (c) of a SubPc/C_{60} organic photodetector. In (c), the thickness of SubPc/C_{60} is 10 nm/40 nm.

Test devices on glass substrates with ITO bottom electrode showed the possibility of obtaining a dark current density in the range of 20 nA/cm^2 at -2 V bias voltage by using low conductivity poly(3,4-ethylenedioxythiophene) (PEDOT) on the anode side and bathocuproine (BCP) on the cathode side. In such a configuration, the photocurrent is still several orders of magnitude higher (Fig. 2) and external quantum efficiency (EQE) exceeds 30% (Fig. 3).

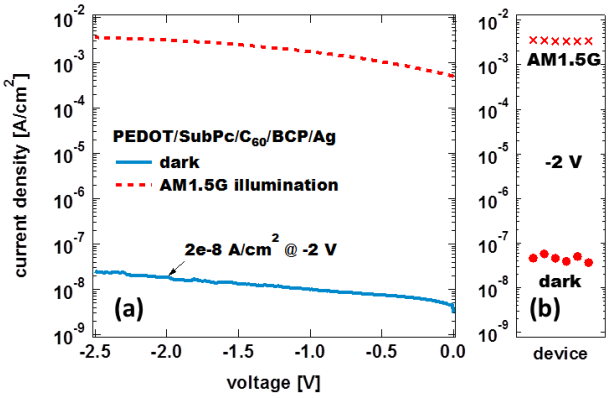

Figure 2. Reverse current density of a SubPc/C_{60} photodiode in dark (blue, solid) and under AM1.5G illumination (red, dashed) (a) and values at -2 V for several devices (b).

Active layer of the photodetector was chosen to match the emission spectrum of typical scintillators. With the SubPc molecule, the absorption peak falls between the wavelengths of 500 and 600 nm (Fig. 3). C_{60} extends this spectrum to 300 nm and provides a sufficient energy band offset for efficient exciton dissociation.

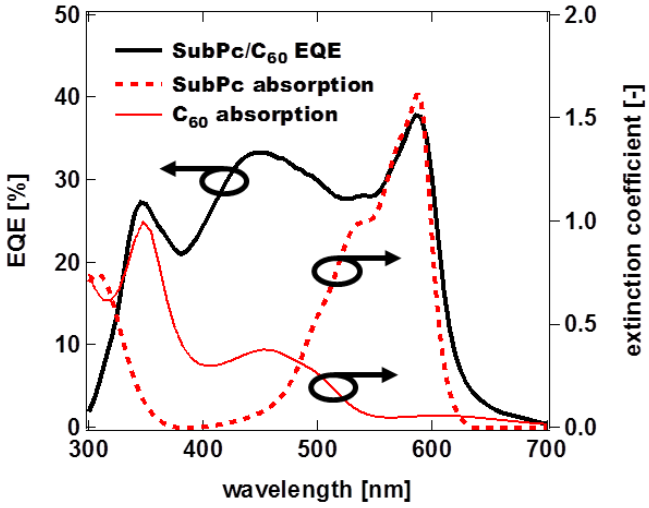

Figure 3. EQE at 0 V bias (black, solid) of a SubPc/C_{60} OPD compared to absorption spectra of pure SubPc (red, dashed) and pure C_{60} (red, solid).

Organic photodiodes were then integrated with a simple organic readout integrated circuit (ROIC), consisting of 1 pentacene thin-film transistor (TFT) per pixel. Pixels of 1 mm and 200 µm pitch were designed with two TFT sizes: 140/70 µm and 70/5 µm width/length, respectively. The layout of the smaller pixel is shown in Fig. 4, with the TFT in the top-right corner. The top metal (Au) of the ROIC acts as the anode of the OPD. Thanks to a semi-transparent cathode (BCP/Ag, 10/10 nm), the devices can be illuminated through the top contact.

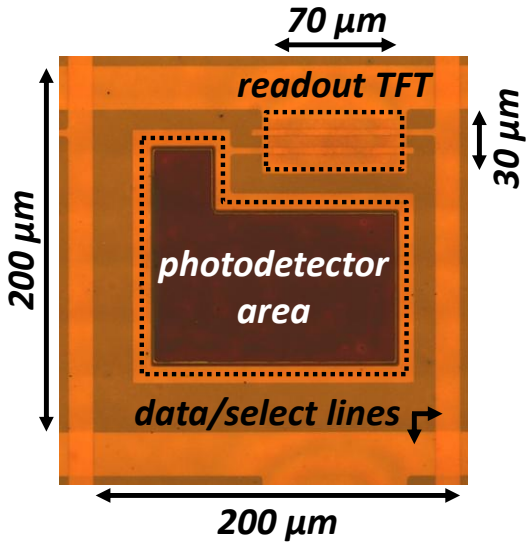

Figure 4. Top view optical micrograph of a single pixel with 200 µm pitch; the readout transistor (effective W/L = 70 µm/5 µm) is in the top-right corner.

Dark signal after integration on the readout backplane was higher than in the test structures due to the bottom MoO_3 layer enabling a fully evaporated OPD stack (Fig. 5). Photosensitivity under top illumination was demonstrated by recording photocurrent under ambient laboratory illumination.

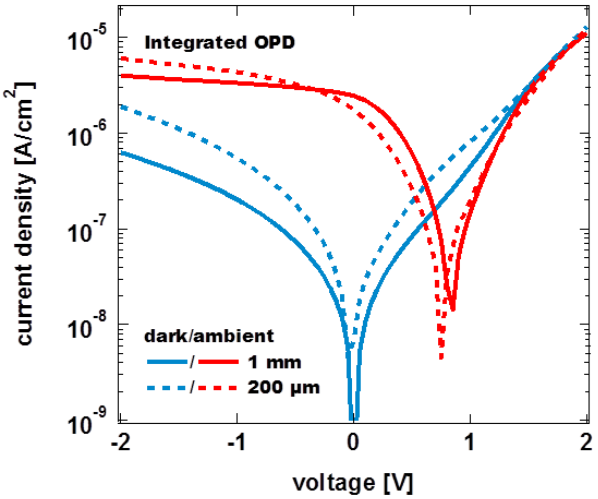

Figure 5. Current-voltage characteristics of OPD pixels after integration in dark (blue) and under ambient laboratory illumination (red) for two pixel sizes (large: solid, small: dashed).

Imagers were fabricated on polyethylene terephthalate (PET) foil laminated atop 6 inch Si wafers. To prevent degradation after deposition of the active layers, fabrication concluded with glass cavity encapsulation of the imagers (Fig. 6, 7). 32x32 pixel focal plane arrays with pixel-to-pixel pitch of 1 mm and 200 µm were designed. Imaging capability was demonstrated by placing shadow objects on top of the encapsulation and illuminating the scene with a calibrated light source. For the array with 1 mm pitch, a checkerboard pattern was used (each square 5 mm wide, Fig. 6a) and for the 200 µm pitch, a circular aperture was detected (5 mm diameter, Fig. 7a). The resulting images clearly matched the shadow mask layouts (Fig. 6b, 7b). Spatial resolution was limited due to light diffusion in the glass cavity of the encapsulation – the distance between the focal plane and the shadow mask was on the order of a millimeter. However, by using printed, thin-film encapsulation, this issue can be eliminated.

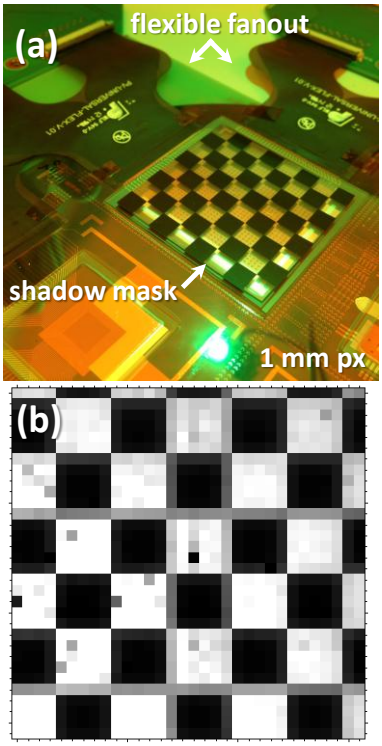

Figure 6. Large imager (1 mm pixel pitch) during characterization using checkerboard shadow mask (a) and the resulting image (b).

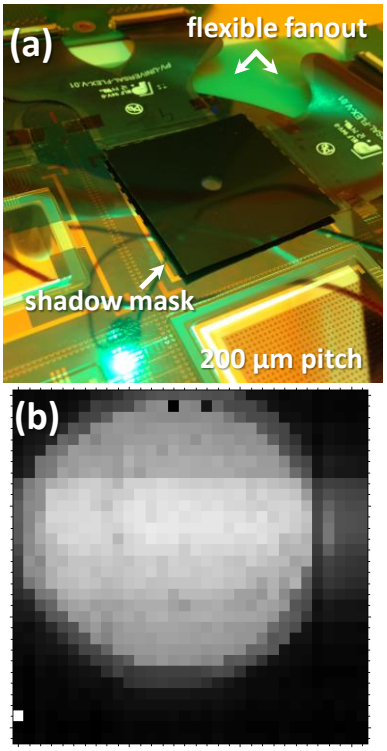

Figure 7. Small imager (200 µm pixel pitch) during characterization using aperture shadow mask (a) and the resulting image (b).

The SubPc/C_{60} imagers had the mean dark current density below 10^{-6} A/cm^2 at -2 V. Under illumination with a 130 µW/cm^2 green LED (λ = 532 nm), the mean photocurrent density was $2 \cdot 10^{-5}$ A/cm^2 with very low spread between the pixels as illustrated in the histogram in Fig. 8. Similar performance was observed for two pixel sizes used.

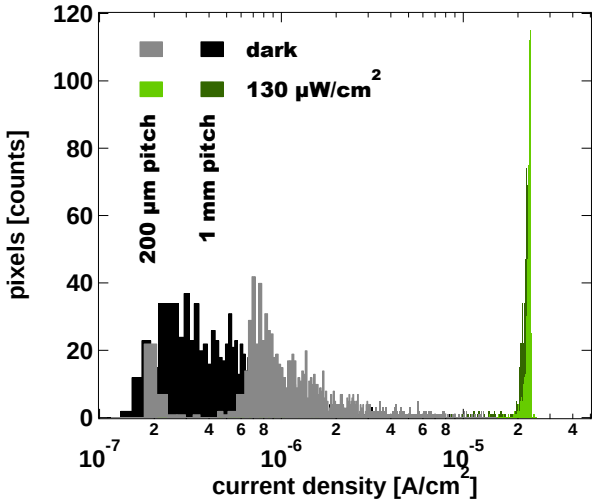

Figure 8. Histograms of dark (gray) and illuminated signal (green) for small (lighter) and large (darker) 32x32 pixel arrays.

Additionally, measurements under illumination with varying incident power were performed using the green LED. Photocurrent measured in the arrays increased linearly from the irradiance of 3 µW/cm^2 up to 130 µW/cm^2 for both pixel sizes (Fig. 9).

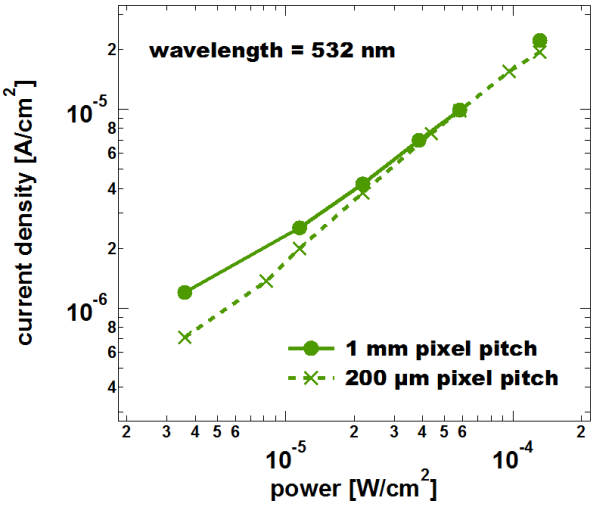

Figure 9. Photocurrent density linearly increasing with the incident power in the range between 3 and 130 µW/cm^2.

The full stack of the imager is shown in Fig. 10. Total thickness of the integrated readout and photodiode is less than 1 µm. The source/drain (S/D) contact of the TFT is at the same time the bottom contact (anode) of the OPD and can be used as a reflector under top illumination. For x-ray detection, a scintillator can be coupled with the imager as the absorption peak of a SubPc active layer matches the output of typical scintillators (550 nm).

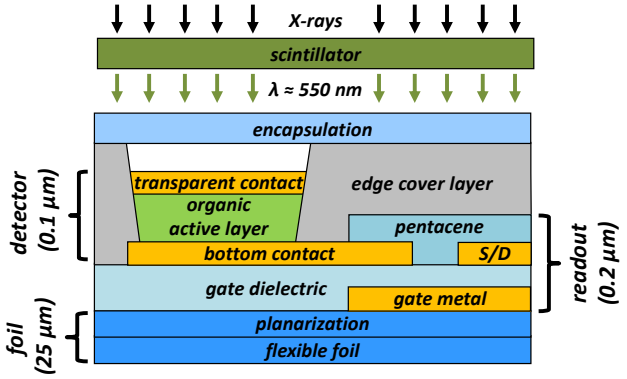

Figure 10. Schematic cross-section of a monolithic imager with organic ROIC and organic photodiode.

By using printed, thin-film encapsulation instead of the glass cavity, the spatial resolution is not compromised by light diffusion and the stack becomes flexible. Imagers can then be delaminated and shaped to a form factor desired in a particular application (Fig. 11).

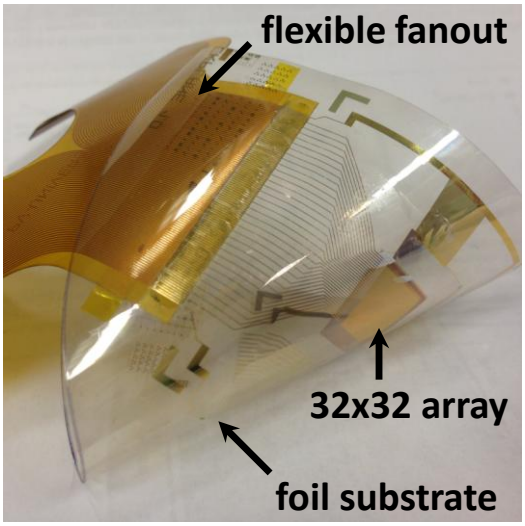

Figure 11. Imager on foil with printed encapsulation layer after delamination from carrier substrate.

The devices demonstrated here show the feasibility of fabricating fully organic imagers with ultrathin active layers on flexible substrates. Easy upscaling of this technology to large-area foil substrates enables ultralight, robust and bendable cameras. One of the possible uses of technology demonstrated as here is x-ray imaging after augmenting the system with a scintillator.

References

[1] OE-A Roadmap for Organic and Printed Electronics, Organic Electronics Association, URL: http://oe-a.vdma.org/en_GB/ (2011).

[2] M. Ihama, H. Inomata, H. Asano, S. Imai, T. Mitsui, Y. Imada, M. Hayashi, T. Gotou, H. Suzuki, D. Sawaki, M. Hamano, T. Nakatani, and Y. Mishima, "CMOS Image Sensor with an Overlaid Organic Photoelectric Conversion Layer," in IISW 2011, pp. 153–156 (2011).

[3] D. Baierl, L. Pancheri, M. Schmidt, D. Stoppa, G.-F. Dalla Betta, G. Scarpa, and P. Lugli, "A hybrid CMOS-imager with a solution-processable polymer as photoactive layer," Nature Communications, vol. 3, p. 1175 (2012).

[4] B. P. Rand, J. Genoe, P. Heremans, and J. Poortmans, "Solar Cells Utilizing Small Molecular Weight Organic Semiconductors," Progress In Photovoltaics: Research And Applications, vol. 15, pp. 659–676, (2007).

[5] H. H. P. Gommans, D. Cheyns, T. Aernouts, C. Girotto, J. Poortmans, and P. Heremans, "Electro-Optical Study of Subphthalocyanine in a Bilayer Organic Solar Cell," Advanced Functional Materials, vol. 17, no. 15, pp. 2653–2658 (2007).